Supporting Information

Jähnichen et al. 10.1073/pnas.1012865107

SI Materials and methods

Materials. DMEM and Ham F-12 medium were obtained from PAA Laboratories, penicillin and streptomycin were obtained from Lonza, phytohemagglutin was obtained from Sigma, and FBS was purchased from Integro. *Myo*-[2-^{3}H]-inositol (10–20 Ci/mmol) and ^{125}I-labeled CXCL12 (2,200 Ci/mmol) were obtained from GE Healthcare and PerkinElmer, respectively. Chemokines were obtained from PeproTech. Iodine 125-labeled nanobodies were obtained using the Iodo-gen method (Pierce) according to the manufacturer's protocol.

cDNA. pCRE/β-gal and pcDNA3.1-CXCR4 were obtained as gifts from C. P. Tensen (Leiden University Medical Center, Leiden, The Netherlands), pcDNA1-HA-mGα_{qi5} was a gift from B. R. Conklin (University of California, San Francisco, CA), and pcDEF$_3$ was a gift from J. A. Langer (Robert Wood Johnson Medical School, Piscataway, NJ). cDNA encoding chemokine receptors CCR5, CCR7, CXCR1, CXCR2, CXCR3, CXCR6, and CXCR7 were obtained from the Missouri University of Science and Technology cDNA Resource Center and were amplified by PCR and subcloned into pcDEF$_3$.

Cell Culture and Transfection. HEK293T, CHO, and COS-7 cells were maintained at 37 °C in a humidified 5% CO_2, 95% air atmosphere in DMEM containing 2 mM *L*-glutamine, 50 IU/mL penicillin, 50 μg/mL streptomycin, and 10% (vol/vol) FCS. Jurkat 3D cells were cultured in a humidified 5% CO_2, 95% air atmosphere in a 1:1 mixture of DMEM and Ham F-12 medium containing 2 mM *L*-glutamine, 50 IU/mL penicillin, 50 μg/mL streptomycin, and 10% (vol/vol) FCS. Cells were transiently transfected with a constant amount of total DNA using DEAE-dextran or linear 25-kDa polyethyleneimine (Polysciences) as carrier as previously described (1).

Immunization, Library Construction, and Selection of Nanobodies. Nanobody libraries were generated using PBMCs isolated from two different llamas immunized six consecutive times with 10^7 HEK293T cells transfected with CXCR4. The nanobody phage library was generated by RT-PCR with at least 10^7 transformants, as previously described (2). The first round of phage display selection was done by using cell membranes from CHO cells overexpressing CXCR4. Membranes were coated onto Maxisorp plates overnight at 4 °C (10 μg in 100 μL PBS solution). The next day, after blocking in 4% milk-PBS solution for 1 h, phages from each library were incubated with the coated membrane in 1% milk-PBS solution and in the presence of a membrane preparation from nontransfected CHO cells (i.e., counterselection). After 2 h, the plates were washed extensively with PBS solution. After washing, bound phages were eluted using trypsin (1 μg/mL) for 15 min at room temperature. Phages were rescued and reamplified in TG1 as usual, giving R1 polyclonal phages. Those R1 phages were used for a second round of selection using membranes from COS-7 cells expressing CXCR4. This unique strategy allows the depletion on non-CXCR4-specific phages. After 2 h incubation, the plates were washed extensively with PBS solution and bound phages were eluted using trypsine (1 μg/mL) for 15 min at room temperature. Phages were rescued in TG1. Individual TG1 colonies were picked up and grown in 96-deep-well plates to produce monoclonal phages after addition of helper phages. The production of monoclonal nanobodies was induced by the addition of isopropyl-β-D-thiogalactopyranoside. The periplasmic fraction containing nanobodies was then prepared by freeze-thawing of the bacterial pellet in PBS solution and subsequent centrifugation to remove cell fragments. For large scale production of nanobodies, the nanobody-encoding cDNA was recloned in the PAX51 expression vector. After overnight induction of a 400 mL bacterial culture with 1 mM isopropyl-β-D-thiogalactopyranoside, the bacteria were pelleted and lysed by freeze-thawing. The pellet was resuspended in PBS solution and centrifuged. The nanobodies were purified from the supernatant containing the periplasm fraction using TALON beads (Clontech Laboratories) according to the manufacturer recommendation and dialyzed against PBS solution.

Competition Binding Assays. Membranes from HEK293T cells transiently expressing CXCR3, CXCR4, or CXCR7 were prepared 48 h after transfection as previously described (1). Periplasms (1:10) or ligands were preincubated with membranes in binding buffer (50 mM Hepes, pH 7.4, 1 mM $CaCl_2$, 5 mM $MgCl_2$, 100 mM NaCl) supplemented with 0.5% BSA for 1 h at 22 °C before the addition of ^{125}I-CXCL12 (40 pM), ^{125}I-238D2 (3 nM), or ^{125}I-238D4 (3 nM) for an additional 2 h at 22 °C. The nonspecific binding was determined in the presence of AMD3100 (3 μM). Membranes were then harvested over polyethylenimine (0.5%)-treated GF/C filter plates (Whatman) and washed three times with ice-cold binding buffer containing 500 mM NaCl. Plates were counted by liquid scintillation.

Inositol Phosphate Accumulation Assay. The nanobody-mediated inhibition of CXCL12-induced inositol phosphate accumulation was determined in *myo*-[2-^{3}H]-inositol-labeled HEK293T cells transiently transfected with pcDNA3.1-CXCR4 and pcDNA1-HA-mGα_{qi5}. In antagonist experiments, the cells were preincubated with test compounds for 1 h before stimulation with CXCL12 (30 nM) for 2 h at 37 °C in the presence of 10 mM LiCl. In agonist experiments, the cells were directly stimulated with test compounds and LiCl (10 mM) for 2 h at 37 °C. The incubation was stopped by aspirating the medium and the addition of ice-cold 10 mM formic acid. The accumulated inositol phosphates were isolated by anion exchange chromatography and counted by liquid scintillation (1).

CRE Reporter Gene Assay. HEK239T cells were transfected with pCRE/β-gal and plasmids (pcDEF$_3$ or pcDNA3.1) encoding the indicated receptors and grown in DMEM supplemented with 10% FCS in 96-well plates. The medium was replaced 32 h after transfection by serum-free DMEM supplemented with 0.5% BSA and ligands as indicated. Following 16 h of ligand incubation, the medium was removed, the cells were lysed in 100 μL of assay buffer (100 mM sodium phosphate buffer, pH 8.0, 4 mM 2-nitrophenol-β-D-pyranoside, 0.5% Triton X-100, 2 mM $MgSO_4$, 0.1 mM $MnCl_2$, and 40 mM β-mercaptoethanol) and incubated at room temperature. The β-gal activity was determined by the measurement of absorption at 420 nm with a Powerwave X340 plate reader (Bio-Tek Instruments).

Chemotaxis Assay. Chemotaxis experiments were performed using ChemoTx plates (Receptor Technologies). Cells were loaded in the upper compartment of the transwell plate and chemotaxis was performed in the presence of CXCL12 and/or test compounds in the lower compartment. For the characterization of antagonistic properties, 12G5 or nanobodies were loaded to the lower compartment and additionally preincubated with the cells in the upper compartment. The chemotaxis chambers were incubated at 37 °C, 100% humidity, and 5% CO_2 for 4 h. The number of cells mi-

grating into each lower compartment were quantified by using calcein AM.

HIV-1 Infection Assays. The CXCR4-using (X4) HIV-1 clone NL4.3 was obtained from the National Institutes of Health/National Institute of Allergy and Infectious Diseases AIDS Reagent program and the CCR5-using (R5) HIV-1 strain BaL was obtained from the United Kingdom Medical Research Council AIDS Reagent Project. The dual-tropic (R5/X4) HIV-1 HE strain was initially isolated from a patient at the University Hospital in Leuven, Belgium (3). The MT-4 cells were seeded out in 96-well plate and the U87 cells in 24-well plates. The test compounds were added at different concentrations together with HIV-1 and the plates were maintained at 37 °C in 5% CO_2. Cytopathic effect induced by the virus was monitored by daily microscopic evaluation of the virus-infected cell cultures. At day 4 to 5 after infection, when strong cytopathic effect was observed in the positive control (i.e., untreated HIV-infected cells), the cell viability was assessed via the in situ reduction of the tetrazolium compound MTS, using the CellTiter 96 AQ_{ueous} One Solution cell proliferation assay (Promega). The absorbance was then measured spectrophotometrically at 490 nm with a 96-well plate reader (Molecular Devices) and compared with four cell control replicates (cells without virus and drugs) and four virus control wells (virus-infected cells without drugs). The IC_{50} (i.e., the drug concentration that inhibits HIV-induced cell death by 50%) was calculated for each compound from the dose–response curve. The 50% cytotoxic concentration of each of the compounds was determined from the reduction of viability of uninfected cells exposed to the agents, as measured by the MTS method described earlier.

PBMCs from healthy donors were isolated by density centrifugation (Lymphoprep; Nycomed) and stimulated with phytohemagglutin for 3 d. The activated cells were washed with PBS solution and viral infections were performed as described previously (4). At 8 to 10 d after the start of the infection, viral p24 Ag was detected in the culture supernatant by ELISA (Perkin-Elmer).

Epitope Mapping of CXCR4 Nanobody Binding Sites. A CXCR4 mutation library was created by random mutagenesis using the shotgun mutagenesis platform from Integral Molecular. A total of 731 clones were generated with all residues mutated at least once (100%), at least twice (98.8%), and 76.2% or 19.9% of the clones presented one or two mutated amino acids, respectively. All mutant CXCR4 were tagged at their N- and C-termini with V5 and Flag epitopes, respectively, allowing detection of cell surface and full-length expression using anti-V5 and anti-Flag antibodies. Nanobodies bound to CXCR4 mutants were detected using an anti-Myc antibody.

Stem Cell Mobilization. All experiments were conducted in strict compliance with European Economic Community and Italian guidelines for laboratory animal welfare. Cynomolgus monkeys were given AMD3100 (1 mg/kg) s.c. at the doses of 1 mg/kg and the nanobody (0.1, 1, 10, or 25 mg/kg) was administered in a single i.v. infusion over a period of 30 min. Mortality, clinical signs, and food consumption were monitored daily. Body weight was recorded once in the pretest period, the day of treatments, and then once weekly. PE-conjugated anti-CD45 and FITC-conjugated anti-CD34 antibodies were used to detect total white blood cells and $CD34^+$ stem cells according to the International Society for Hematotherapy and Graft Engineering protocol (5–7).

Data Analysis and Presentation. Concentration response curves were fitted to the Hill equation using an iterative, least-squares method (Prism 4.0; GraphPad) to provide EC_{50} or IC_{50} values. Competition binding affinities and functional antagonist affinities (i.e., K_i) were calculated using the Cheng and Prusoff equation (8). Antagonist affinities were optionally expressed as K_B values using the method of Arunlakshana and Schild (9). Results were compared using Student *t* test or one-way analysis of variance followed by a Bonferroni-corrected *t* test for stepwise comparison when multiple comparison was made. *P* values lower than 0.05 were considered to be significant.

1. Verzijl D, et al. (2008) Noncompetitive antagonism and inverse agonism as mechanism of action of nonpeptidergic antagonists at primate and rodent CXCR3 chemokine receptors. *J Pharmacol Exp Ther* 325:544–555.
2. Roovers RC, et al. (2007) Efficient inhibition of EGFR signaling and of tumour growth by antagonistic anti-EFGR Nanobodies. *Cancer Immunol Immunother* 56:303–317.
3. Pauwels R, et al. (1990) Potent and selective inhibition of HIV-1 replication in vitro by a novel series of TIBO derivatives. *Nature* 343:470–474.
4. Schols D, et al. (1997) Inhibition of T-tropic HIV strains by selective antagonization of the chemokine receptor CXCR4. *J Exp Med* 186:1383–1388.
5. Barnett D, et al.; General Haematology Task Force of the British Committee for Standards in Haematology (1999) Guideline for the flow cytometric enumeration of CD34+ haematopoietic stem cells. Prepared by the CD34+ haematopoietic stem cell working party. *Clin Lab Haematol* 21:301–308.
6. Gratama JW, et al.; European Working Group on Clinical Cell Analysis (1998) Flow cytometric enumeration of CD34+ hematopoietic stem and progenitor cells. *Cytometry* 34:128–142.
7. Sutherland DR, Anderson L, Keeney M, Nayar R, Chin-Yee I International Society of Hematotherapy and Graft Engineering (1996) The ISHAGE guidelines for CD34+ cell determination by flow cytometry. *J Hematother* 5:213–226.
8. Cheng Y, Prusoff WH (1973) Relationship between the inhibition constant (K1) and the concentration of inhibitor which causes 50 per cent inhibition (I50) of an enzymatic reaction. *Biochem Pharmacol* 22:3099–3108.
9. Arunlakshana O, Schild HO (1997) Some quantitative uses of drug antagonists. 1958. *Br J Pharmacol* 120(4 suppl):151–161.

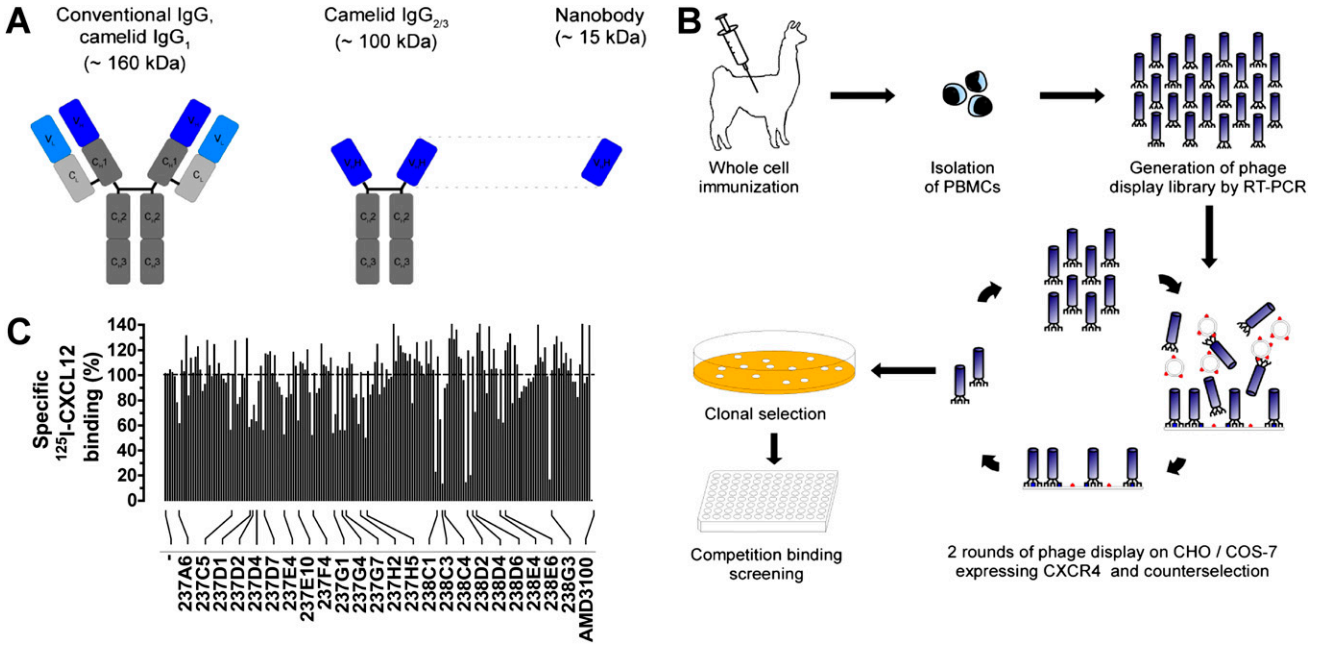

Fig. S1. Schematic overview over the generation procedure of competitively antagonistic nanobodies against CXCR4. (*A*) Schematic structural organization of a conventional four-chain antibody compared with a camelid heavy chain-only antibody and a nanobody derived from camelid heavy chain-only antibodies. (*B*) Llamas were immunized with whole HEK293T cells transiently transfected with CXCR4. A phage library was generated from the RNA extracted from isolated PBMCs. After two rounds of selection and deselection with CHO and COS-7 cells transfected with CXCR4 and mock-transfected, respectively, phages expressing potential CXCR4-specific monoclonal nanobodies were isolated and purified. Periplasmic extracts were then screened in a ^{125}I-CXCL12 displacement assay. (*C*) Screening of periplasmic fractions (1:10) in a ^{125}I-CXCL12 competition assay on cell membranes of HEK293T cells transiently expressing CXCR4. The AMD3100 was taken as positive control.

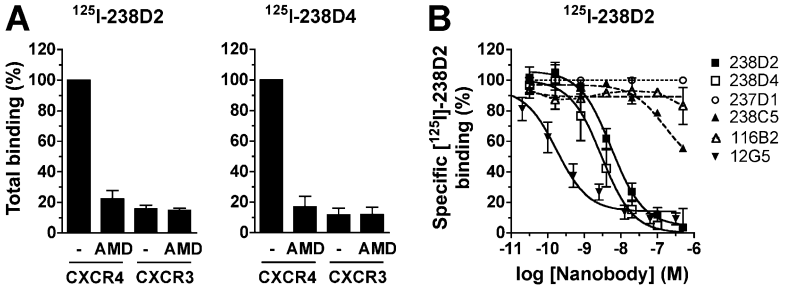

Fig. S2. Characterization of monovalent CXCR4 nanobodies. (*A*) Binding assay of radiolabeled ^{125}I-238D2 and ^{125}I-238D4 nanobodies on membranes of HEK293T transiently transfected with CXCR4 or CXCR3. (*B*) Displacement assay of ^{125}I-238D2 with CXCR4 nanobodies and the CXCR4-specific monoclonal antibody 12G5.

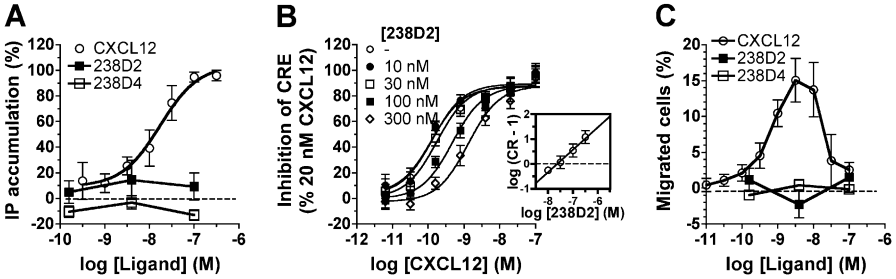

Fig. S3. The monovalent nanobody 238D2 is a competitive antagonist for CXCR4. (*A*) Measurement of inositol phosphates (IP) production in HEK293T cells transfected with CXCR4 and $G\alpha_{qi5}$ indicate that CXCL12 possesses agonistic activity whereas 238D2 and 238D4 show no agonism. (*B*) HEK293T cells transfected with CXCR4 together with the pCRE/β-gal reporter gene display CRE activation upon CXCL12 stimulation. The 238D2 nanobody shows competitive antagonism and Schild–Plot analysis (*Inset*) was performed by establishing concentration response curves for CXCL12 in the presence of increasing concentrations of 238D2. Data are shown as means ± SEM (n = 4–6). (*C*) Chemotaxis experiment of Jurkat cells show that CXCL12, but not 238D2 or 238D4, acts as an agonist.

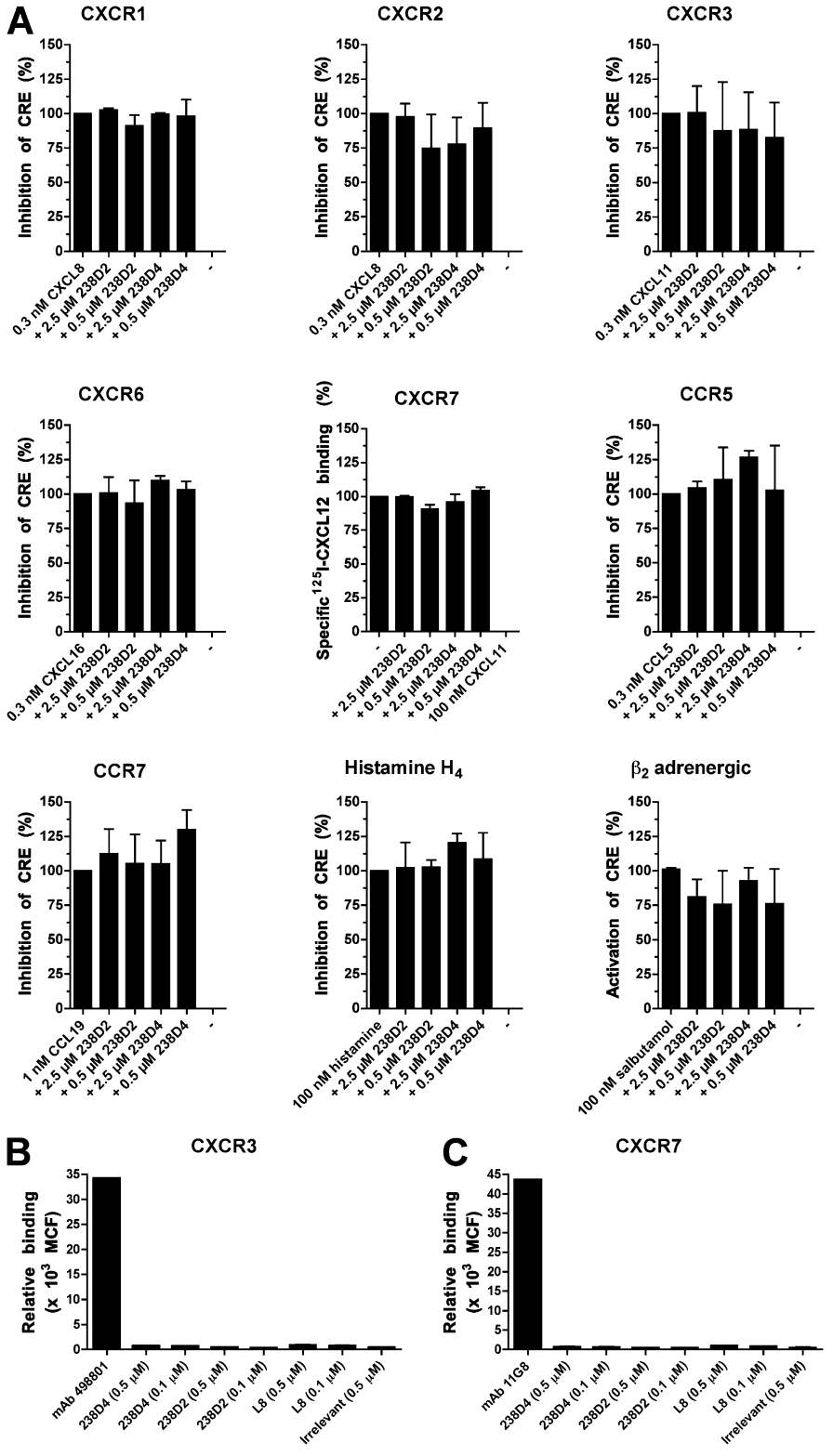

Fig. S4. The monovalent nanobodies 238D2 and 238D4 do not act on chemokine receptors CCR5, CCR7, CXCR1, CXCR2, CXCR3, CXCR6, CXCR7 or β_2 adrenergic and histamine H_4 receptors. (*A*) The selectivity screen was performed with two concentrations of 238D2 and 238D4 in the presence of an EC_{50}–EC_{80} concentration of an agonist and in the absence (for endogenously expressed β_2 adrenoreceptors) or the presence of forskolin (3 μM; for all other receptors) on HEK293T cells transiently transfected with cDNA encoding the indicated receptors using a CRE/β-gal reporter gene assay. The selectivity of the nanobodies for CXCR4 over CXCR7 was tested in a competition binding assay on membranes from HEK293T cells transiently expressing CXCR7 using ^{125}I-CXCL12 (50 pM) as radioligand. Data are shown as means ± SEM (n = 2–4). (*B* and *C*) Transiently transfected HEK293T cells expressing CXCR3 (*B*) or CXCR7 (*C*) were incubated in the presence of specific monoclonal antibodies (498801 and 11G8 for CXCR3 and CXCR7, respectively) or with two different concentrations of CXCR4-specific nanobodies 238D2, 238D4, and L8. An irrelevant nanobody was taken along as a negative control. Cell-bound nanobodies were detected by flow cytometry using appropriate conjugated secondary antibodies. Data are shown as means ± SEM (n = 4, from two independent experiments). MCF, mean channel fluorescence.

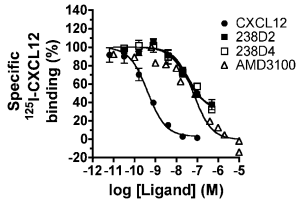

Fig. S5. The monovalent nanobodies 238D2 and 238D4 bind to the constitutively active mutant CXCR4-N3.35A. Competitive binding experiment of ^{125}I-CXCL12 on membranes of HEK293T cells transfected with the constitutively active mutant of CXCR4, CXCR4-N3.35A, in the presence of cold CXCL12, AMD3100, or the monovalent nanobodies 238D2 or 238D4.

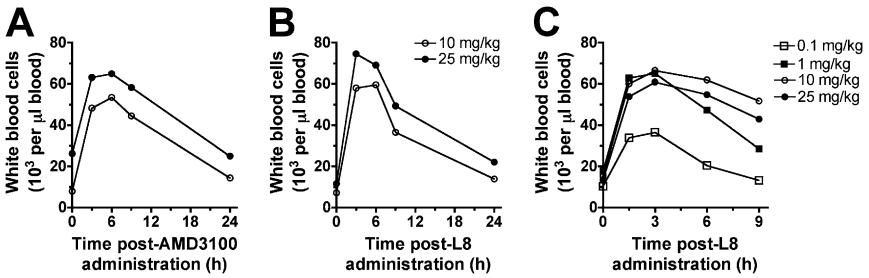

Fig. S6. CXCR4-specific biparatopic nanobody L8 induces WBC mobilization in vivo to a similar extent as AMD3100. (*A*) Two independent monkeys were injected s.c. with 1 mg/kg of the CXCR4-specific antagonist AMD3100 and blood samples were taken over a period of 24 h after administration. (*B*) Two independent monkeys were injected i.v. with the biparatopic CXCR4-specific nanobody L8 at 10 mg/kg or 25 mg/kg. Blood samples were taken over a period of 24 h after administration. (*C*) Four independent monkeys were injected i.v. with various amounts of L8 nanobody, namely 0.1 mg/kg, 1 mg/kg, 10 mg/kg, or 25 mg/kg. Blood samples were withdrawn up to 9 h after administration. In all experiments, the presence of WBCs was determined by flow cytometry analysis.

Table S1. Receptor affinity and maximal displacement of ^{125}I-CXCL12, ^{125}I-238D2, and ^{125}I-238D4 for monovalent nanobodies and CXCR4 reference ligands

	^{125}I-CXCL12		^{125}I-238D2		^{125}I-238D4	
Nanobody	Displacement, %	K_i, nM	Displacement, %	K_i, nM	Displacement, %	K_i, nM
238D2	93	9.8	97	3.9	105	5.9
238D4	99	6.0	101	1.6	103	2.8
237A6	0	>500	0	>500	0	>500
237D1	0	>500	0	>500	0	>500
237D2	0	>500	0	>500	0	>500
237G7	0	>500	0	>500	0	>500
238C5	0	>500	45*	>100	38*	>100
116B2[†]	0	>500	0	>500	0	>500
AMD3100	94	38.9	102	18.2	99	45.7
12G5	54[‡]	0.65	89[‡]	0.22	90[‡]	0.49

The experiments were performed on membranes from HEK293T cells transiently expressing CXCR4. Data were shown as arithmetic (displacement) or geometric means (K_i) from two to six independent experiments.
*Maximum not reached at the highest test concentration of 0.5 μM, displacement at 0.5 μM.
[†]Control nanobody.
[‡]Significantly different from 100% (95% CIs are 32–76%, 83–95% and 87–93%, respectively).

Table S2. CXCR4 amino acids identified as critical residues in the binding of 238D2 and 238D4

				Nanobody		
Residue/clone	Mutation	V5	Flag	238D2	238D4	12G5
S178						
2396	S178C	79.1 ± 22.7	66.5 ± 21.6	44.9 ± 13.4	28.2 ± 14.0*	91.8 ± 16.7
709	P163L, S178I	130.2 ± 30.9	81.2 ± 26.9	64.1 ± 19.6	30.0 ± 24.0*	113.0 ± 41.4
1057	K230E, S178R	83.9 ± 8.3	95.2 ± 14.0	54.6 ± 5.8	11.4 ± 20.1*	111.6 ± 41.3
E179						
414	C218R, E179V, S351T	32.2 ± 17.3	95.8 ± 17.4	71.1 ± 6.7	8.0 ± 20.4*	−9.1 ± 24.5*
2834	E179V, G258E	62.4 ± 16.3	87.1 ± 8.3	84.6 ± 7.8	19.5 ± 21.6*	1.5 ± 5.8*
D187						
3728	D187A, Y157C	95.0 ± 7.3	92.6 ± 16.5	77.1 ± 18.2	−16.4 ± 14.8*	95.1 ± 30.0
2084	D187V	121.9 ± 20.4	94.7 ± 17.2	93.6 ± 5.2	−8.0 ± 7.6*	89.5 ± 10.6
F189						
1129	F189V	72.4 ± 33.1	96.1 ± 22.8	−1.9 ± 24.2*	5.2 ± 27.1*	94.7 ± 16.7
913	F189S, K308R	108.1 ± 10.7	96.8 ± 35.1	−32.6 ± 18.7*	−16.9 ± 19.9*	110.5 ± 28.5
465	F189L, S319P, V155E	105.7 ± 9.2	53.0 ± 39.6	31.8 ± 16.2*	12.2 ± 18.9*	50.4 ± 25.6
P191						
2184	P191T	127.6 ± 22.0	107.4 ± 16.0	15.8 ± 5.4*	123.9 ± 21.1	117.9 ± 26.8
N192						
914	N192K	60.9 ± 10.5	68.1 ± 8.4	8.3 ± 3.6*	55.8 ± 12.7	57.7 ± 51.7
W195						
3630	W195R	102.1 ± 6.0	92.4 ± 16.9	10.0 ± 10.4*	58.8 ± 7.7	85.5 ± 26.6
V196						
2270	V196E	131.7 ± 22.0	92.8 ± 16.5	20.6 ± 32.9*	94.0 ± 23.8	96.8 ± 11.7
E277						
185	E277A, I245V, N298S	111.0 ± 24.8	91.6 ± 11.7	35.5 ± 12.3*	69.3 ± 36.9	93.9 ± 22.1
3622	E277G	151.7 ± 23.7	73.2 ± 11.3	19.5 ± 11.9*	52.5 ± 20.4	61.3 ± 34.9

CXCR4 mutants tagged with V5 or Flag at their N terminus and C terminus, respectively, were used to determine the binding of the nanobodies 238D2 or 238D4 or the monoclonal antibody 12G5. Critical amino acids in clones containing more than one mutation were differentiated by comparing the reactivity of other clones with mutation of the same residues. Critical amino acids for nanobody 238D2 were identified under high stringency assay conditions (mutations of F189 affect binding of 238D2 at both high and low stringency). Results from three independent immunofluorescence experiments.

*Mutants presenting a loss of binding to 238D2 and 238D4 nanobodies or 12G5 antibody.